

**UNCLASSIFIED**

**Defense Technical Information Center  
Compilation Part Notice**

**ADP011735**

**TITLE:** THz Sources Based on Semiconductor Quantum Structures

**DISTRIBUTION:** Approved for public release, distribution unlimited

This paper is part of the following report:

**TITLE:** International Conference on Terahertz Electronics [8th], Held in Darmstadt, Germany on 28-29 September 2000

To order the complete compilation report, use: ADA398789

The component part is provided here to allow users access to individually authored sections of proceedings, annals, symposia, etc. However, the component should be considered within the context of the overall compilation report and not as a stand-alone technical report.

The following component part numbers comprise the compilation report:

**ADP011730 thru ADP011799**

**UNCLASSIFIED**

# THz Sources Based on Semiconductor Quantum Structures

K. Unterrainer, J. Ulrich, R. Zobl, G. Strasser, and E. Gornik

**Abstract** – We present a study on spontaneous THz emission from semiconductor quantum structures. THz emission from parabolically graded AlGaAs/GaAs quantum wells driven by an in-plane electric field has been measured. We have analyzed the grating coupled radiation in the temperature range from 20 K to 240 K. The peak emission corresponds to the intersubband plasmon in the parabolic potential. From a quantum cascade structure we observe spontaneous THz emission, based on carrier injection into the excited state of a 26 nm quantum well. We have measured luminescence at a photon energy of 17.3 meV with a full linewidth at half maximum of 1.3 meV.

## I. INTRODUCTION

For the development of electrically driven semiconductor sources emitting in the far-infrared wavelength region several concepts have been pursued. A far-infrared laser based on radiative transitions of holes in p-doped Germanium between Landau levels was demonstrated /1/. Sources operating without a magnetic field can be constructed employing intersubband transitions in heterostructures. THz intersubband electroluminescence

has been observed in parabolic quantum wells /2/, in superlattices /3/, and more recently in quantum cascade structures /4,5/.

We studied the electroluminescence from two different structures. The first structure is a parabolically graded quantum well and the second one is a quantum cascade structure.

## II. THZ EMISSION FROM PARABOLIC QUANTUM WELLS

Parabolic quantum wells are promising candidates for THz sources operating above liquid nitrogen temperature, because their emission frequency is independent of the electron distribution and concentration in the well. In absorption and emission spectroscopy [6], coupling between the radiation and the electron system has been observed at only one frequency. This is the harmonic oscillator frequency, solely determined by the width and the energetic depth of the quantum well. These observations confirmed the validity of the generalized Kohn theorem [7] in parabolic quantum wells, stating that long wavelength radiation (as compared to the width of the well) only couples to the center of mass co-ordinate

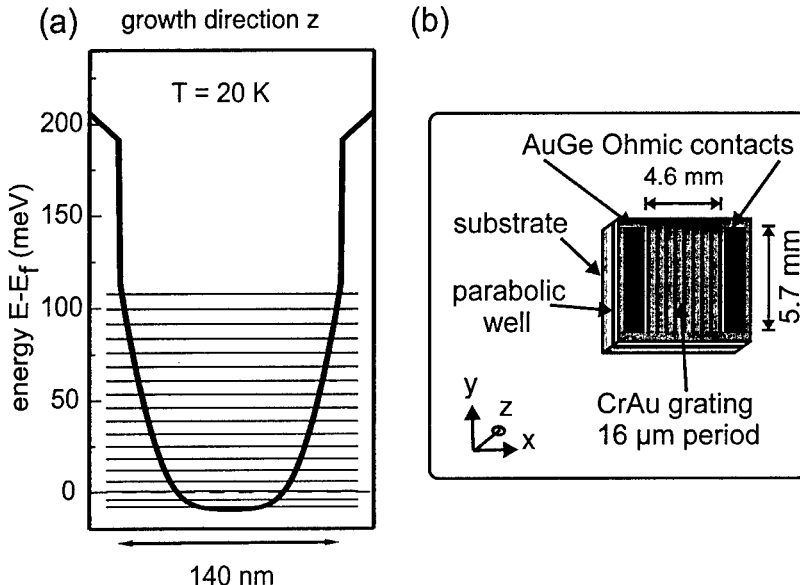


Fig.1: a) Self-consistent calculation of the band diagram of the 140 nm well. The horizontal lines denote the energy levels in the graded part of the well. b) Device geometry of the 140 nm well sample.

K. Unterrainer, J. Ulrich, and R. Zobl are with the Institut für Festkörperelektronik, G. Strasser and E. Gornik are with the Mikrostrukturzentrum, Technische Universität Wien, A-1040 Wien, Austria.

of an electron system confined in a parabolic potential.

Two samples were examined: one with 140 nm, the other one with 200 nm well width, both with 167 meV energetic well depth. The samples were grown by molecular beam epitaxy using a digital alloy technique.

The electron concentration in both wells was determined by Hall measurements. In the 140 nm well, the electron concentration varies from  $3.8 \times 10^{11} \text{ cm}^{-2}$  at 20 K to  $5.1 \times 10^{11} \text{ cm}^{-2}$  at 240 K. In the 200 nm well, the corresponding values are  $2.7 \times 10^{11} \text{ cm}^{-2}$  at 20 K,  $3.4 \times 10^{11} \text{ cm}^{-2}$  at 240 K. The energy band diagram of the 140 nm well is displayed in Fig. 1a.

Fig. 1b shows the device geometry schematically. The wells are contacted with two AuGe Ohmic contact stripes. In order to couple out the intersubband radiation, that is polarized with its electrical field perpendicular to the layers, a metallic CrAu grating of 16  $\mu\text{m}$  (50  $\mu\text{m}$ ) period, with its stripes parallel to the contacts, was evaporated between the contacts.

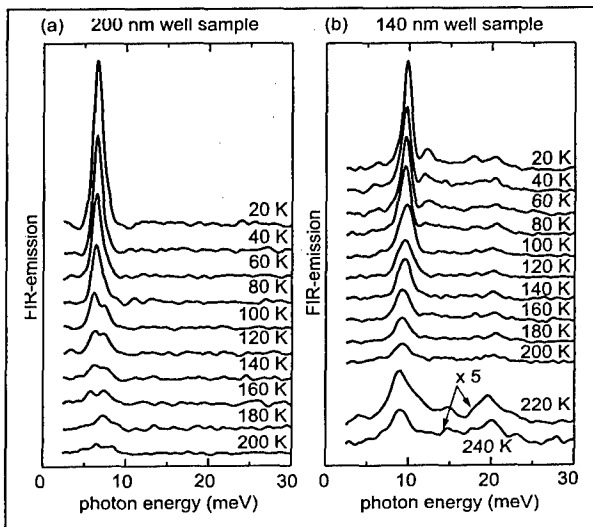


Fig. 2: Emission spectra a) of the 200 nm well sample and b) of the 140 nm well sample for various temperatures as indicated. The spectra of the two highest temperatures in (b) are shown enlarged by a factor of five.

We measured the electroluminescence of the parabolic quantum wells using a Fourier-transform infrared spectrometer in the step scan mode with a spectral resolution of 0.5 meV. The sample was mounted on the cold finger of a helium-flow cryostat. The emitted radiation was collected by an off-axis parabolic mirror with an f/2 aperture, transmitted through the spectrometer, and then focussed on a helium cooled Si-bolometer. The whole beam path was purged with dry nitrogen gas to minimize the far-infrared absorption by water vapor. The electron gas in the well was excited by application of a pulsed electric field between the Ohmic contacts at a frequency of 411 Hz and 50 % duty cycle. A lock-in amplifier was employed to detect the bolometer signal.

In Fig. 2a, spectra of the 200 nm well at various temperatures are displayed. The peak emission is observed at a photon energy of 6.6 meV for all temperatures. This value corresponds to the harmonic oscillator energy, calculated from the well dimensions as 6.0 meV. In agreement with the generalized Kohn theorem, the emission energy is unaltered by the temperature-induced variation of the electron distribution in the well. The spectra of the 140 nm well in Fig. 2b

show a 20 K emission peak at 9.8 meV (calculated as 8.4 meV) that is slightly shifted to lower energies (9.1 meV), as the temperature is raised up to 240 K. The full width at half maximum of the emission line of both samples ranges from 1 meV at low temperatures ( $T < 100$  K) to 2 meV in the high temperature regime ( $T > 100$  K) /8/.

### III. TERAHERTZ-ELECTROLUMINESCENCE IN A QUANTUM CASCADE STRUCTURE

Investigations of intersubband electroluminescence /3,4,5/ have been performed aiming at an electrically driven coherent terahertz emitter based on intersubband transitions. In the mid-infrared wavelength region a quantum cascade laser has been demonstrated by Faist et al. /9/. We are trying to downscale the concept for emission of radiation with a photon energy below the LO-phonon energy in GaAs (36 meV). In that case, the upper state lifetime is not limited by LO-phonon scattering.

Our structure is made up of 50 periods of a chirped Al<sub>0.15</sub>Ga<sub>0.85</sub>As/GaAs superlattice, as seen in Fig. 3. The radiative transition occurs in the widest (26 nm) quantum well. At an appropriate electric field (22 mV/period), electrons are resonantly injected from the first miniband of the injector (4 wells) into the second state ( $E_2$ ) of the transition well. The electrons escape from the ground state ( $E_1$ ) via fast resonant tunneling whereas tunneling from  $E_2$  downstream is inhibited by the minigap of the adjacent injector. The second miniband at the operation bias is Wannier-Stark localized and does not contribute to carrier transport. The two center wells of the injector are lightly doped ( $n = 1 \times 10^{16} \text{ cm}^{-3}$ ) to insure a constant electric field across the structure.

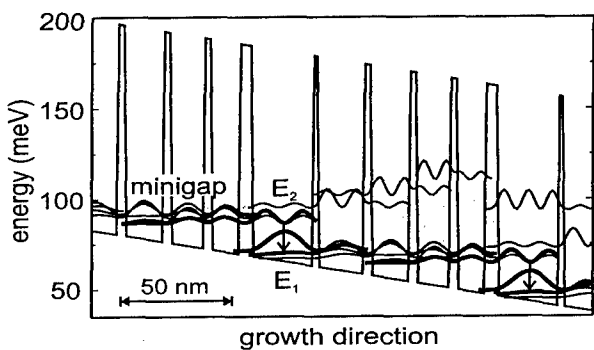


Fig. 3: Part of the band structure of a quantum cascade structure designed for emission of terahertz radiation. It has been calculated by selfconsistently solving Schrödinger's and Poisson's equation.

The layer system is grown by molecular beam epitaxy on an n+ doped substrate that is used as the electrical bottom contact. One sample (1300  $\mu\text{m} \times 250 \mu\text{m}$ ) was prepared with a 16  $\mu\text{m}$  period Au-grating on top that serves as the electrical top contact and as the optical outcoupler at the same time. In a second sample with a larger period grating (50  $\mu\text{m}$ ) the layer system was removed between the Au-stripes by reactive ion etching, leaving 7 ridges of

1300  $\mu\text{m}$  length and 25  $\mu\text{m}$  width emitting radiation from the edges.

In order to detect the terahertz luminescence of the samples we have employed two different spectrometers. The first one is the Fourier spectrometer described in the previous section. Our second electroluminescence set-up contains an InSb-cyclotron resonance detector which is tunable by a magnetic field. The sample is located in a second magnet in order to screen the field. The radiation is guided from the sample to the detector in a closed light pipe. The whole optics is immersed in liquid He, so that room temperature background radiation cannot reach the detector nor the sample.

We observe terahertz-emission at 17.3 meV as displayed in Fig 4. This is consistent with the calculated energy difference  $E_2 - E_1$  of 17.1 meV. The linewidth is 1.3 meV, see Fig 4 (a). The linewidth of 2.2 meV in the InSb-detector spectra in Fig 4 (b) is not the true linewidth of our sample because the InSb-detector has an intrinsic linewidth of 1.5 meV. We do not observe emission from transitions other than  $E_2 - E_1$ . There is a monotonous increase of signal with the injection current up to the breakup of the first miniband. The increase of light output with current is sublinear. This is an indication /5/ that the non-radiative scattering rate increases with the injection current and with the population of the  $E_2$  excited state, as it is the case for electron-electron- or Auger-scattering processes.

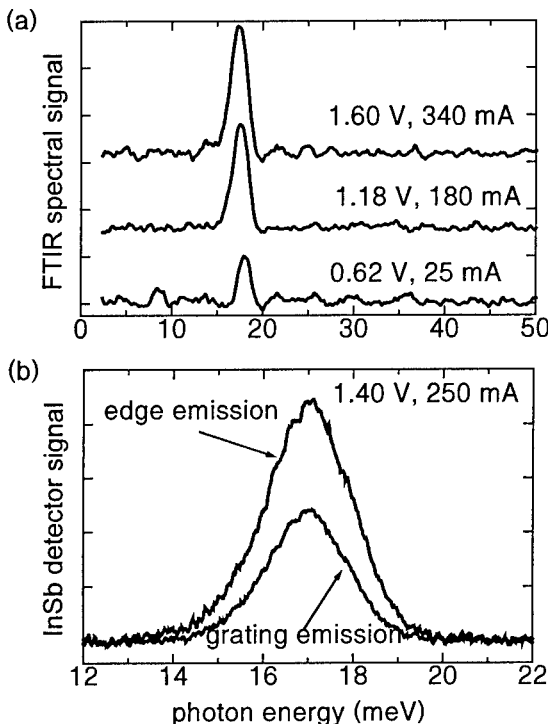


Fig. 4: (a) Emission spectra recorded with the Fourier-transform spectrometer at three different biases. (b) Emission spectra recorded with the InSb-detector spectrometer, comparing grating coupled and edge emission at the same current.

In spite of the advantages of the FTIR-spectrometer over

the InSb-setup, i. e. the high spectral resolution (0.25 meV) the large spectral range (0 - 50 meV), we have used the InSb-setup for its higher signal to noise ratio and for the absence of distortion of the signal by room temperature background radiation. The comparison of the two differently processed samples shown in Fig. 4 (b) yields: The edge outcoupling is about twice as efficient as the grating coupled surface emission. We attribute this difference to strong absorption in the highly doped top contact layer /10/.

#### IV. CONCLUSION

We have demonstrated electrically driven THz emission of parabolic quantum wells up to a temperature of 240 K. At high temperatures, the thermal energy  $k_B T$  exceeds the photon energy by a factor greater than two. The electron distribution in thermal equilibrium varies significantly in the temperature range of interest. However, we observe single frequency emission, and the impact of high temperatures on the frequency and the line shape is small. The emission efficiency is limited by the temperature dependent decrease of intersubband life time. From the quantum cascade structures we observe a narrow (1.3 meV) spontaneous emission line at 17.3 meV. The efficiency of edge emission is higher than that of grating coupled emission.

#### Acknowledgement

This work has been supported by the Austrian Science Foundation (START Y47, Wittgenstein Award) and by the EU-TMR Program (INTERACT).

#### References

1. K. Unterrainer, C. Kremser, E. Gornik, C. R. Pidgeon, Y. L. Ivanov, E. E. Haller; Phys. Rev. Lett. 53, 1714 (1988).
2. K. D. Maranowski, A. C. Gossard, K. Unterrainer, E. Gornik; Appl. Phys. Lett. 69, 3522 (1996).
3. M. Helm, P. England, E. Colas, F. DeRosa, S. J. Allen, Jr.; Phys. Rev. Lett. 63, 74 (1988).
4. B. Xu, Q. Hu, M. R. Melloch, Appl. Phys. Lett. 71, 440 (1997).
5. M. Rochat, J. Faist, M. Beck, U. Oesterle, M. Illegems, Appl. Phys. Lett. 73, 3724 (1998).
6. A. Wixforth, M. Kaloudis, C. Rocke, K. Ensslin, M. Sundaram, J. H. English, A. C. Gossard; Semicond. Sci. Technol. 9, 215 (1994).
7. L. Brey, N. F. Johnson, B. I. Halperin Phys. Rev. B 40, 647 (1989).
8. J. Ulrich, R. Zobl, K. Unterrainer, G. Strasser, E. Gornik, K.D. Maranowski, A.C. Gossard; Appl. Phys. Lett. 74, 3158 (1999).
9. J. Faist, F. Capasso, D. L. Sivco, C. Sitori, A. L. Hutchinson, A. Y. Cho, Science 264, 553 (1994)
10. J. Ulrich, R. Zobl, K. Unterrainer, G. Strasser, E. Gornik; "Magnetic field enhanced quantum cascade emission"; Appl. Phys. Lett. 76, 19 (2000).